Phononic crystal diffraction gratings

Rayisa P. Moiseyenko, Sarah Herbison, Nico F. Declercq, and Vincent Laude

Citation: J. Appl. Phys. **111**, 034907 (2012); doi: 10.1063/1.3682113
View online: http://dx.doi.org/10.1063/1.3682113
View Table of Contents: http://jap.aip.org/resource/1/JAPIAU/v111/i3
Published by the American Institute of Physics.

Phononic crystal diffraction gratings

Rayisa P. Moiseyenko,[1,2,a)] Sarah Herbison,[2] Nico F. Declercq,[2] and Vincent Laude[1]
[1]*Institut FEMTO-ST, Université de Franche-Comté and CNRS, 32 avenue de l'Observatoire, F-25044 Besançon Cedex, France*
[2]*Georgia Institute of Technology, UMI Georgia Tech - CNRS, George W. Woodruff School of Mechanical Engineering, Georgia Tech Lorraine, 2 rue Marconi, 57070 Metz-Technopole, France*

(Received 15 September 2011; accepted 4 January 2012; published online 10 February 2012)

When a phononic crystal is interrogated by an external source of acoustic waves, there is necessarily a phenomenon of diffraction occurring on the external enclosing surfaces. Indeed, these external surfaces are periodic and the resulting acoustic diffraction grating has a periodicity that depends on the orientation of the phononic crystal. This work presents a combined experimental and theoretical study on the diffraction of bulk ultrasonic waves on the external surfaces of a 2D phononic crystal that consists of a triangular lattice of steel rods in a water matrix. The results of transmission experiments are compared with theoretical band structures obtained with the finite-element method. Angular spectrograms (showing frequency as a function of angle) determined from diffraction experiments are then compared with finite-element simulations of diffraction occurring on the surfaces of the crystal. The experimental results show that the diffraction that occurs on its external surfaces is highly frequency-dependent and has a definite relation with the Bloch modes of the phononic crystal. In particular, a strong influence of the presence of bandgaps and deaf bands on the diffraction efficiency is found. This observation opens perspectives for the design of efficient phononic crystal diffraction gratings. © *2012 American Institute of Physics*. [doi:10.1063/1.3682113]

I. INTRODUCTION

The study of phononic crystals (PC) has generated much interest in recent years. Phononic crystals are the acoustical analogs of photonic crystals for optical waves.[1] A PC can be generally defined as a one-, two-, and three-dimensional periodic structure that is composed of at least two different materials that possess a significant mismatch in their elastic properties.[2–4] The periodic scattering and internal reflections on the boundaries of inclusions contained in the unit-cell lead to strong spectral and spatial dispersion of acoustic waves. One of the most interesting characteristics of PCs is their ability to exhibit bandgaps, which are finite frequency regions for which sound propagation in or through the crystal is prohibited in one or more specific wave vector directions. Bandgap locations and widths mainly depend on the materials employed in the crystal construction, the lattice geometry, and the size and shape of any inclusions.[5,6]

Phononic crystals are sometimes classified according to the materials that form the host matrix and the periodic lattice inclusions (e.g., fluid-solid, solid-solid, etc.). The term sonic crystal is sometimes used in the literature to refer to a structure where the host material of the crystal is a fluid and the material used for the inclusions is a solid, especially if the host fluid is air and the frequency range under study is in the audible, i.e., sonic, range.[7–10] This terminology is also sometimes employed when the host fluid is water.[11] However, since the frequencies studied in this work are in the ultrasonic range and the term phononic crystal is more generally applied in the literature, this term will be employed in this work.

Generally speaking, frequency bandgaps originating from Bragg interference occur for definite wavelengths as compared to the pitch of the periodic structure; for instance $\lambda \approx a/2$ for square lattice PC. Many works have focused on studying the absence of transmission of certain frequencies through the crystal or on guiding effects that can occur when defects or waveguides are introduced into the crystal structure.[12,13] Defining a transmission (and a reflection) unambiguously clearly requires that a single propagating mode exists in the medium surrounding the PC. Propagation inside the PC remains monomodal for frequencies below the diffraction cut-off, which is related to the pitch of the PC and depends on the direction of observation.[14] Above the PC diffraction cut-off, the existence of orders of diffraction inside the crystal has to be taken into account for any quantitative analysis. Furthermore, because any practical implementation necessarily requires a crystal of finite size, the diffracted fields that may be generated by the exterior surfaces play an important role. Indeed, we should expect the surface of the PC to behave as a diffraction grating since it is a periodic structure as was observed for surface acoustic waves.[15] Previous theoretical studies conducted on layers of tubes that were assumed to behave as acoustic diffraction gratings also support this view.[16] In addition to the PC diffraction cut-off frequency, the previous discussion leads us to define a diffraction grating cut-off frequency for acoustic waves propagating in the surrounding medium. The apparent periodicity of the PC diffraction grating clearly varies depending on the orientation of the plane that defines the crystal boundary. With b the apparent periodicity, the grating law is observed for an incident and diffracted plane waves[17]

a)Author to whom correspondence should be addressed. Electronic mail: rayisa.moiseyenko@georgiatech-metz.fr.

$$\sin\theta_m + \sin\theta_i = m\frac{V}{fb}, \tag{1}$$

with V the velocity of acoustic waves in the surrounding medium, f the frequency, and m the index of the considered diffraction order.

In this paper, we consider phononic crystals from the perspective of acoustic diffraction gratings and we study the relations between phononic properties of the interior of the PC—bandgaps and deaf bands—and diffraction at its boundaries. We are particularly interested in finding ways to influence diffraction efficiency via the phononic properties of the crystal. The paper is organized as follows. First, we describe the particular water-steel PC we have studied and the experimental setups we have employed for measurements. Transmission results are compared with band structures of the infinite periodic crystal computed with a finite element model (FEM). Experimental diffraction results are then presented and compared to FEM computations for finite phononic crystals. Finally, we end with a discussion of the significance of the results.

II. EXPERIMENTAL SETUP FOR TRANSMISSION AND DIFFRACTION MEASUREMENTS

The phononic crystal used in this work is identical to the one studied by Hsiao *et al.*,[18] but the measurement frequency range is different. The PC is composed of an array of steel rods arranged according to a triangular lattice. The rods have a diameter $d = 1.2$ mm and the distance between two rods is $a = 1.5$ mm, which defines the pitch of the periodic structure. Two support plates were perforated with a computer-controlled tooling machine to define the triangular lattice. The rods are inserted in the support plates which guarantees alignment with good accuracy. Measurements are performed with the PC immersed in a water tank with a polar/C-scan ultrasonic apparatus, as depicted in Fig. 1. Two different orientations of the phononic crystal are considered, corresponding to the directions ΓK and ΓM of the first Brillouin zone, as depicted in Figs. 1(a) and 1(b), respectively.

In order to measure the transmission, an emitting transducer and a receiving transducer are positioned on a fork and aligned normally to the crystal surface. Measuring the transmission here means measuring the diffraction efficiency of the transmitted wave of zeroth diffraction order. For diffraction measurements, the emitting transducer is fixed and aligned normally to the crystal surface, but the receiving transducer is mounted in a rotating fork attached to the polar/C-scan robot, and aimed at the point on the crystal surface where the emitter is incident. The center of rotation of the receiver is set to be even with the crystal surface. Angular scans are performed where waveforms are collected at many angles within the diffracted field on the incident side. Such measurements hence give information on the reflected waves with diffraction orders larger than one. Frequency analysis is then performed on the waveforms in order to determine the frequencies present in the field as a function of the angle. For practical reasons, the angular range for all diffraction measurements is 40°, from 20° to 60° with respect to the normal to the crystal surface. It should be noted that due to the geometry of the polar/C-scan robot, the diffraction measurements are taken just beyond the second crystal support plate, whereas the transmission measurements are taken for the region of the crystal between the two support plates, which is a better configuration to guarantee the periodicity of the rods of the crystal.

In order to cover a wide range of frequencies, two pairs of transducers are used. One pair has a nominal center

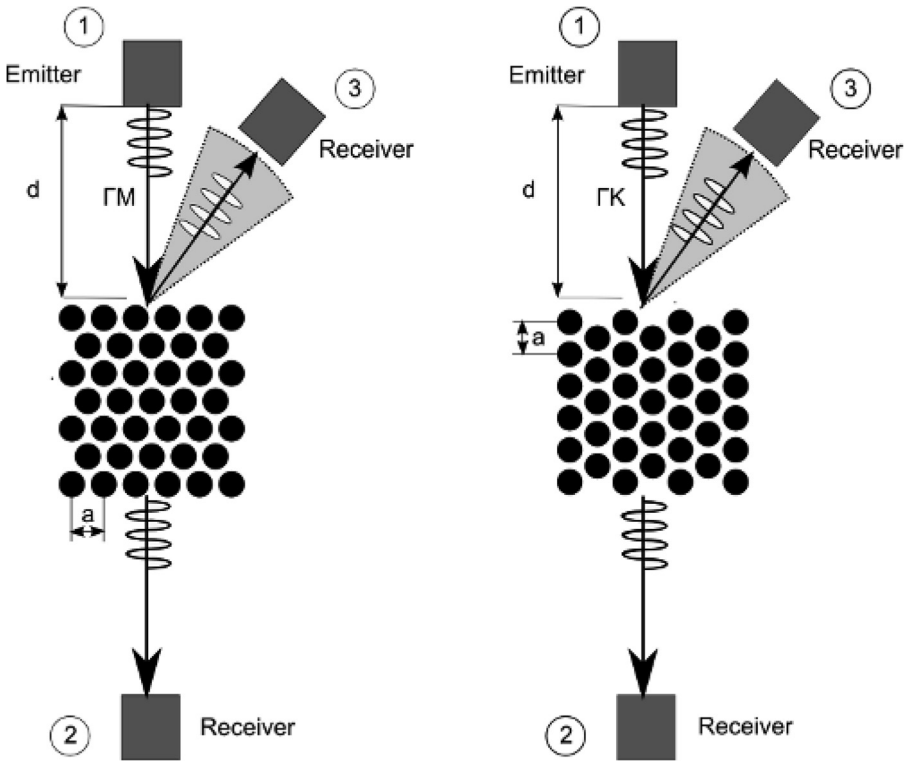

FIG. 1. Experimental setup for diffraction and transmission measurements in (left) the ΓM and (right) the ΓK directions of the phononic crystal. The apparent diffraction grating periodicity is (left) $b = a$ and (right) $b = \sqrt{3}a$.

frequency of 1 MHz (Valpey-Fisher IS0104GP), and the other has a nominal center frequency of 2.25 MHz (Technisonics ISL-0203-SP). The beam width of all transducers is approximately 10 mm. The frequency spectra of the transmission measured for both transducer pairs are shown in Fig. 2. As can be seen, there is a missing range of frequencies between 1.5 and 1.8 MHz where no accurate measurement can be taken. All measurements taken using pulses are obtained with 16 averages and are normalized with respect to the spectra obtained between the transducer pairs in the absence of the crystal. All data are sampled at 200 MHz. The angular resolution for angular scans is 0.1°.

III. TRANSMISSION AND DIFFRACTION MEASUREMENTS

The band structure of the phononic crystal is calculated using the finite element method and is presented in Fig. 3(a) for the ΓK direction and in Fig. 4(a) for the ΓM direction. This band structure is essentially the same as in Ref. 18. The presence of frequency bandgaps has been highlighted in these diagrams so that a direct comparison with the measured transmissions in Figs. 3(b) and 4(b) can be made. It can be observed that the transmission is always less than unity, which is not surprising since part of the incident energy is reflected and diffracted back toward the incident half space. An absence of transmission is observed as expected for any frequency that falls inside a theoretical bandgap. However, there are other frequency ranges where a very low transmission is observed though bands are theoretically predicted to exist. This phenomenon is discussed in detail in Ref. 18, though measurement frequencies are limited to values below 1.2 MHz, and attributed to the fact that such bands are indeed deaf. Deafness means that the relevant Bloch wave is antisymmetric with respect to the propagation direction, with the consequence that a symmetrical incident plane wave is unable to transfer its energy to the Bloch wave. Interestingly, the same phenomenon was observed recently for Lamb waves in phononic crystal plates.[19] Deaf bands are identified carefully by checking the symmetry of the Bloch waves supported by each band in Figs. 3(a) and 4(a), and appear as dotted lines in these diagrams, whereas symmetrical (non deaf) bands appear as solid lines.

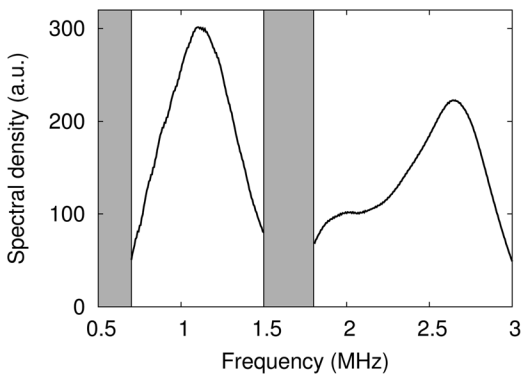

FIG. 2. Experimental transmission as a function of frequency (in arbitrary units) for the two pairs of transducers. These measurements are used to normalize transmission and diffraction measurements in the presence of the phononic crystal.

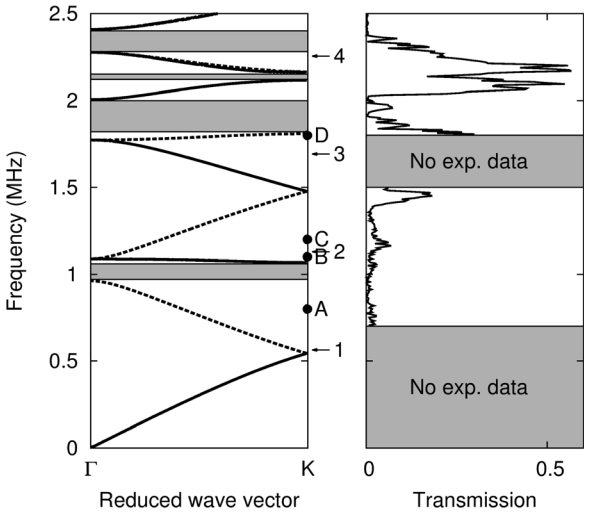

FIG. 3. (Left) Phononic band structure in the ΓK direction of a triangular-lattice phononic crystal composed of steel rods in water, with parameters $a = 1.5$ mm and $d = 1.2$ mm. Frequency bandgaps appear in gray. Cut-off frequencies for diffraction orders in water are indicated with arrows ($b = \sqrt{3}a$). (Right) Experimental transmission through the phononic crystal.

From Eq. (1), the cut-off frequency for every diffraction order in water can be estimated for normal incidence as

$$f_m = m\frac{V}{b}, \tag{2}$$

with $b = a$ (1.5 mm) and $\sqrt{3}a$ (2.6 mm) in the ΓM and in the ΓK directions, respectively. The cut-off frequencies for the first diffraction orders have been indicated with arrows on Figs. 3(a) and 4(a).

Measurements of the diffraction efficiency of waves diffracted toward the incident medium are shown in Fig. 5. These dispersion diagrams show the dispersion relation of the diffracted waves, in the form frequency as a function of propagation angle, with the additional information of the diffraction efficiency represented as a gray scale. The

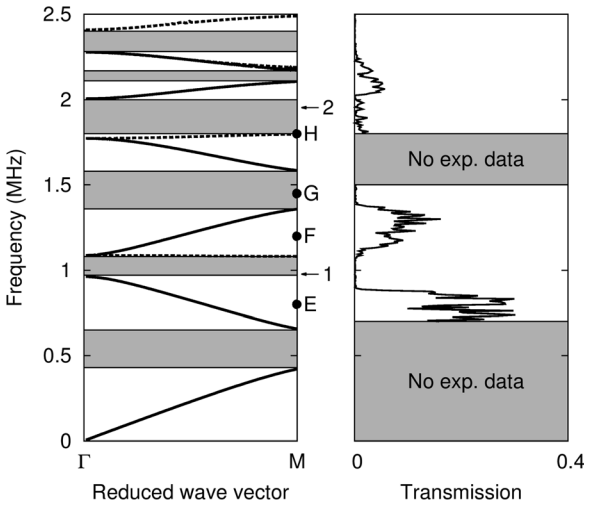

FIG. 4. (Left) Phononic band structure in the ΓM direction of a triangular-lattice phononic crystal composed of steel rods in water, with parameters $a = 1.5$ mm and $d = 1.2$ mm. Frequency bandgaps appear in gray. Cut-off frequencies for diffraction orders in water are indicated with arrows ($b = a$). (Right) Experimental transmission through the phononic crystal.

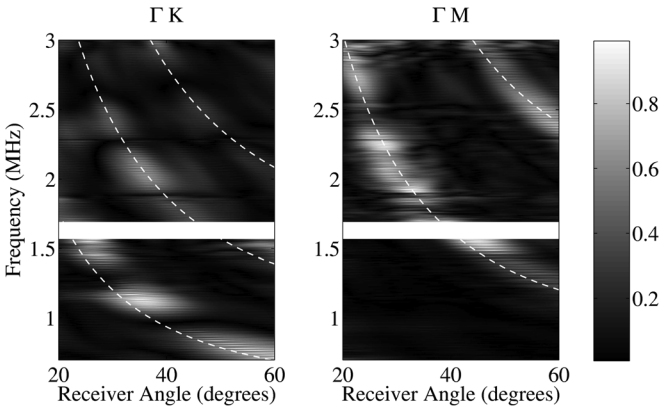

FIG. 5. Experimentally determined diffraction efficiency as a function of propagation angle and frequency, normalized to unity.

theoretical dispersion relations, given by Eq. (1), have been added to the diagrams as dotted lines. It can be seen that the diffracted energy clearly concentrates along dispersion lines, which is a direct experimental validation of the model of the phononic crystal diffraction grating. The experimental angular distribution of energy has a finite extent around each dispersion line due to the natural dispersion of sound columns in water. This distribution could be concentrated by using transducers with a larger area, emitting and receiving sound beams with a distribution closer to the ideal plane wave case.

The measurements clearly indicate a strong dependence of the diffraction efficiency with frequency. In a traditional acoustic diffraction grating, there is also a dependence of the diffraction efficiency with frequency, that ultimately depends on the shape of the corrugation of the diffracting surface.[20] However, the dependence is smoother in the latter case and abrupt variations as seen on the phononic crystal grating case are not the rule.

Examining the first diffraction order efficiency in the ΓK direction, there are two maxima around 0.75 MHz and 1.1 MHz. In the theoretical band structure in Fig. 3(a), the phononic crystal supports only deaf bands at these frequencies. Furthermore, the experimental transmission in Fig. 3(b) is close to zero at both frequencies. We then formulate the hypothesis that the increased diffraction efficiency at these frequencies could be related to the quenching of transmission resulting from the phononic crystal deafness. This logical connection, however, is not reflexive, since there is a frequency range between 1.2 and 1.4 MHz where the diffraction efficiency is low while the crystal supports only a deaf band. Furthermore, the bandgap around 1 MHz is not concomitant with an increased diffraction efficiency. Examining the second diffracted order, there is low diffraction efficiency between 1.7 and 1.95 MHz (bandgap range) and increased diffraction efficiency between 1.95 and 2.15 MHz (transmission range).

Examining the first diffraction order efficiency in the ΓM direction, we see that it remains low from 1.2 to 1.45 MHz and abruptly increases afterwards, just as the third bandgap is entered. Unfortunately, no experimental data are available from 1.5 to 1.8 MHz. Above 1.8 MHz, the diffraction efficiency is always high, while at the same time the transmission in Fig. 4(b) remains low. Between 2.35 and 2.6 MHz, diffraction is mostly to the second rather than to the first diffraction order.

IV. FINITE ELEMENT DIFFRACTION MODEL

In order to explore the connection between diffraction at the phononic crystal surface and the phononic properties of its interior, a specific FEM is built. Elastic waves inside the steel rods and acoustic waves in water are accounted for through a fluid-structure weak form FEM implementation.[21] At the interface between fluid and solid, a boundary condition relating the pressure in the fluid to the normal acceleration of the solid boundary is imposed. Conversely, the traction acting on the solid boundary is taken as the pressure exerted by the fluid. A unidirectional emission transducer is modeled as a source of pressure waves in the form of a rectangular solid with three clamped sides and a prescribed normal acceleration on the fourth side. Since we consider a finite phononic crystal and an external source of waves, the finite computational domain has to be terminated with radiation boundary conditions to avoid unwanted reflections. Considering that the scattering of incident plane waves on small cylindrical objects results mostly in cylindrical waves in the far field, a cylindrical radiation boundary condition located on a circular boundary centered on the phononic crystal is used.

Figures 6 and 7 present examples of computed pressure fields for the ΓK and the ΓM directions, respectively. The

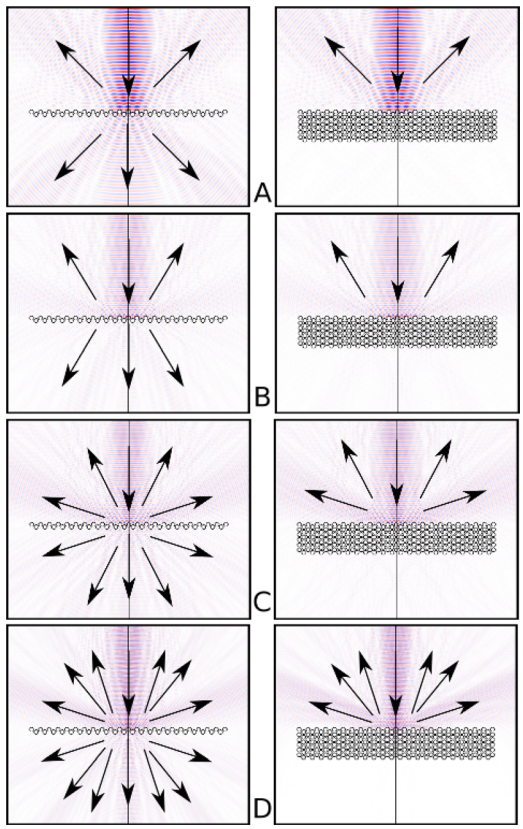

FIG. 6. (Color online) Finite element computation of the pressure distribution for a source emitting plane wavelike sound incident normally on the phononic crystal oriented in the ΓK direction. A two-layer (left side) and a 12-layer (right side) phononic crystal is considered. Computations are shown for the frequencies labeled A (0.8 MHz), B (1.1 MHz), C (1.2 MHz), and D (1.8 MHz) in Fig. 3.

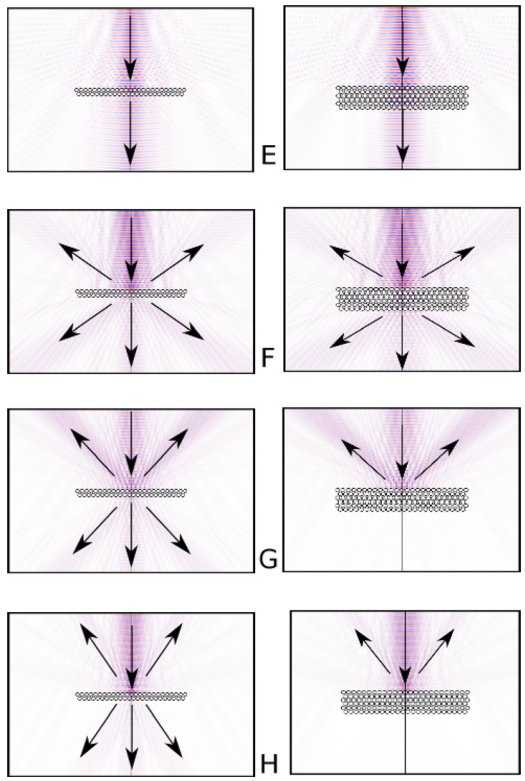

FIG. 7. (Color online) Finite element computation of the pressure distribution for a source emitting plane wavelike sound incident normally on the phononic crystal oriented in the ΓM direction. A two-layer (left side) and a 6-layer (right side) phononic crystal is considered. Computations are shown for the frequencies labeled E (0.8 MHz), F (1.2 MHz), G (1.45 MHz), and H (1.8 MHz) in Fig. 4.

real part of the pressure field is displayed and normalized to range between −1 and +1. Two different cases are considered: a two-layer phononic crystal, and a 12-layer phononic crystal (respectively, 6-layer phononic crystal) for the ΓK direction (resp., for the ΓM direction). By considering two values for the number of layers, we wish to highlight the effect of the formation of bandgaps and deaf bands on diffraction.

For the ΓK orientation, Figs. 6 and 4 frequencies are selected from the band structure in Fig. 3(a). At frequency point A (0.8 MHz), the phononic crystal is deaf and only first diffraction orders are propagating in water. It can be observed that the 12-layer phononic crystal does not transmit to any diffraction order through the crystal, in contrast to the 2-layer PC. Second diffraction orders switch from evanescent to propagating in between frequency points B (1.1 MHz) and C (1.2 MHz). For this frequency range, the PC is again deaf, causing the incident energy to be solely reflected or diffracted backwards. At frequency point D (1.8 MHz), third diffraction orders are propagating and the PC is deaf again.

For the ΓM orientation, Figs. 7 and 4 frequencies are further selected from the band structure in Fig. 4(a). At frequency point E (0.8 MHz), only reflection and transmission to the zeroth diffraction orders can occur. First diffraction orders are propagating at frequency points F (1.2 MHz), G (1.45 MHz), and H (1.8 MHz). At point F, transmission through the PC is allowed, and all diffraction orders receive a part of the incident energy. Point G is inside the third BG for the ΓM direction, and rather efficient diffraction to the backward first diffraction order is observed. In contrast, point H is also inside a BG for the ΓM direction (the fourth BG), but a low diffraction efficiency is obtained.

V. CONCLUSION

In this paper, we have considered phononic crystals from the perspective of the diffraction of incoming plane waves on the crystal boundaries. As usual, there are certain frequency ranges within which incoming waves cannot pass through the crystal, with the physical origin of this phenomenon arising either from the occurrence of phononic bandgaps or from phononic deafness. However, in contrast to previous papers insisting on the characterization of bandgaps and deaf bands by transmission measurements or computations, we have found that the backward reflected energy distributes among available diffraction orders. We found that the dispersion of the diffraction orders depends solely on the apparent periodicity of the boundary enclosing the PC, while the diffraction efficiencies depend in a complicated fashion on the phononic properties of the inside of the PC. It is also important to note that bandgaps and deaf bands need only be directional here, since no defects are inserted inside the phononic crystal, in contrast to the case of phononic cavities and waveguides. Though the particular phononic crystal we have considered was not especially designed to operate as an efficient acoustic diffraction grating, we could find some frequencies for which the diffraction efficiency of selected diffraction orders is indeed significantly increased. This work opens the way toward the design of efficient phononic crystal gratings. By clever optimization of the periodic structure, we conjecture that configurations can be found with diffraction efficiencies approaching 100% for a chosen diffraction order.

ACKNOWLEDGMENTS

Financial support by the Agence Nationale de la Recherche under grant ANR-09-BLAN- 0167-01 is gratefully acknowledged.

[1]E. Yablonovitch, Phys. Rev. Lett. **58**, 2059 (1987).
[2]M. S. Kushwaha, P. Halevi, L. Dobrzynski, and B. Djafari-Rouhani, Phys. Rev. Lett. **71**, 2022 (1993).
[3]M. Kafesaki, R. S. Penciu, and E. N. Economou, Phys. Rev. Lett. **84**, 6050 (2000).
[4]Y. Tanaka, Y. Tomoyasu, and S.-i. Tamura, Phys. Rev. B **62**, 7387 (2000).
[5]X.-Z. Zhou, Y.-S. Wang, and C. Zhang, J. Appl. Phys. **106**, 014903 (2009).
[6]C. M. Reinke, M. F. Su, R. H. Olsson III, and I. El-Kady, Appl. Phys. Lett. **98**, 061912 (2011).
[7]L.-Y. Wu and L.-W. Chen, J. Phys. D **44**, 045402 (2011).
[8]R. Martínez-Sala, J. Sancho, J. V. Sánchez, V. Gómez, J. Llinares, and F. Meseguer, Nature **378**, 241 (1995).
[9]F. Cervera, L. Sanchis, J. Sánchez-Pérez, V. R. Martínez-Sala, C. Rubio, and F. Meseguer, Phys. Rev. Lett. **88**, 023902 (2002).
[10]J. O. Vasseur, P. A. Deymier, A. Khelif, P. Lambin, B. Djafari-Rouhani, A. Akjouj, L. Dobrzynski, N. Fettouhi, and J. Zemmouri, Phys. Rev. E **65**, 056608 (2002).
[11]M. Torres, F. R. Montero de Espinosa, D. Garcia-Pablos, and N. Garcia, Phys. Rev. Lett. **82**, 3054 (1999).
[12]A. Khelif, A. Choujaa, B. Djafari-Rouhani, M. Wilm, S. Ballandras, and V. Laude, Phys. Rev. B **68**, 214301 (2003).

[13]F. R. Montero de Espinosa, E. Jimenez, and M. Torres, Phys. Rev. Lett. **80**, 1208 (1998).
[14]V. Laude, Y. Achaoui, S. Benchabane, and A. Khelif, Phys. Rev. B **80**, 092301 (2009).
[15]K. Kokkonen, M. Kaivola, S. Benchabane, A. Khelif, and V. Laude, Appl. Phys. Lett. **91**, 083517 (2007).
[16]C. Rubio, D. Caballero, J. Sánchez-Pérez, R. Martinez-Sala, J. Sanchez-Dehesa, F. Meseguer, and F. Cervera, J. of Lightwave Technology **17**, 2202 (1999).
[17]E. G. Loewen and E. Popov, *Diffraction Gratings and Applications* (Marcel-Dekker, New York, 1997).
[18]F.-L. Hsiao, A. Khelif, H. Moubchir, A. Choujaa, C.-C. Chen, and V. Laude, J. Appl. Phys. **101**, 044903 (2007).
[19]M. Gorisse, S. Benchabane, G. Teissier, C. Billard, A. Reinhardt, V. Laude, E. Defaÿ, and M. Aïd, Appl. Phys. Lett. **98**, 234103 (2011).
[20]D. R. Wirgin, A. J. Opt. Soc. Am. **59**, 1348 (1969).
[21]*Comsol Multiphysics, Acoustics Module, User's Guide, Version 3.5a*. (2008).